NEUROSCIENCE
RESEARCH ARTICLE

Allison R. Peterson, D.K. Binder / Neuroscience 411 (2019) 185–201

Regulation of Synaptosomal GLT-1 and GLAST during Epileptogenesis

Allison R. Peterson and Devin K. Binder*

Center for Glial-Neuronal Interactions, Division of Biomedical Sciences, School of Medicine, University of California, Riverside, CA, USA

Abstract—Astrocytes regulate extracellular glutamate homeostasis in the central nervous system through the Na^+-dependent glutamate transporters glutamate transporter-1 (GLT-1) and glutamate aspartate transporter (GLAST). Impaired astrocyte glutamate uptake could contribute to the development of epilepsy but the regulation of glutamate transporters in epilepsy is not well understood. In this study, we investigate the expression of GLT-1 and GLAST in the mouse intrahippocampal kainic acid (IHKA) model of temporal lobe epilepsy (TLE). We used immunohistochemistry, synaptosomal fractionation and Western blot analysis at 1, 3, 7 and 30 days post-IHKA induced status epilepticus (SE) to examine changes in GLT-1 and GLAST immunoreactivity and synaptosomal expression during the development of epilepsy. We found a significant upregulation in GLT-1 immunoreactivity at 1 and 3 days post-IHKA in the ipsilateral dorsal hippocampus. However, GLT-1 immunoreactivity and synaptosomal protein levels were significantly downregulated at 7 days post-IHKA in the ipsilateral hippocampus, a time point corresponding to the onset of spontaneous seizures in this model. GLAST immunoreactivity was increased in specific layers at 1 and 3 days post-IHKA in the ipsilateral hippocampus. GLAST synaptosomal protein levels were significantly elevated at 30 days compared to 7 days post-IHKA in the ipsilateral hippocampus. Our findings suggest that astrocytic glutamate transporter dysregulation could contribute to the development of epilepsy.

Key words: glutamate transporter-1, GLT-1, astrocyte, seizure, kainic acid, epilepsy.

INTRODUCTION

Epilepsy is a group of neurological disorders characterized by the occurrence of unprovoked seizures (Fisher et al., 2014). Epilepsy is a major public health problem that affects more than 70 million people worldwide, with approximately 2.4 million people diagnosed with epilepsy each year (Ngugi et al., 2010; Singh and Trevick, 2016). Temporal lobe epilepsy (TLE) is the most common form of epilepsy with focal seizures, and is frequently associated with resistance to currently available pharmacological treatments. Approximately 30% of patients taking antiepileptic drugs (AEDs) still have seizures (Kwan and Brodie, 2000), thus there is a need for new therapeutic approaches that could potentially treat patients with drug-resistant epilepsies (Jutila et al., 2002).

Current AEDs work primarily by targeting neurons through modulation of ion channels, enhancement of inhibitory neurotransmission, or attenuation of excitatory neurotransmission. Newer AEDs still primarily target neurons but through novel mechanisms *e.g.* binding to the SV2A protein on presynaptic vesicles (Sankaraneni and Lachhwani, 2015). Suppression of neurotransmission can consequently lead to psychiatric and behavioral side effects which are common undesired effects associated with AEDs (Chen et al., 2017). Adverse effects to AEDs can lead to poor adherence and AED discontinuation in up to 30% of patients (Bootsma et al., 2009). Thus, there is a need for alternative pharmacological approaches with fewer deleterious side effects for the treatment of epilepsy.

Astrocytes are a critical component of the tripartite synapse, where they are involved in the active control of neuronal activity and synaptic neurotransmission (Araque et al., 1999). Astrocytes are also involved in ion homeostasis, regulation of extracellular space volume and clearance of neurotransmitters (Araque et al., 2014). Astrocytic glutamate transporters are key components in the regulation of neuronal transmission. Glutamate transporter-1 (GLT-1) and glutamate aspartate transporter (GLAST) are part of a family of Na^+-dependent transporters responsible for

*Corresponding author at: 1247 Webber Hall, Division of Biomedical Sciences, School of Medicine, University of California, Riverside, CA, 92521, USA.
E-mail address: dbinder@ucr.edu (Devin K. Binder).
Abbreviations: AEDs, Antiepileptic drugs; CNS, central nervous system; DAPI, 4′,6-diamidino-2-phenylindole; EEG, electroencephalogram; GFAP, glial fibrillary acidic protein; GLAST, glutamate aspartate transporter; GLT-1, glutamate transporter-1; GCL, granule cell layer; HSP90, heat shock protein 90; KDa, kilodalton; SE, status epilepticus; SLM, stratum lacunosum moleculare.

https://doi.org/10.1016/j.neuroscience.2019.05.048

regulating extracellular glutamate homeostasis in the central nervous system (CNS). GLT-1 and GLAST transporters are primarily found on astrocytes and are the most common glutamate transporters associated with excitatory synapses (Kim et al., 2011). GLT-1 is responsible for the majority of extracellular glutamate clearance from the synaptic cleft and is essential for excitatory neurotransmitter balance (Tanaka et al., 1997). We have previously discovered that changes in GLT-1 expression occur during epileptogenesis in the intrahippocampal kainic acid (IHKA) model of epilepsy (Hubbard et al., 2016).

In this study, we aimed to further our understanding of astrocytic glutamate transporters by quantitatively examining changes in GLT-1 and GLAST protein regulation during epileptogenesis. The IHKA mouse model of temporal lobe epilepsy was used (Levesque and Avoli, 2013) together with immunohistochemical analysis, synaptosomal fractionation, and Western blot analysis at 1, 3, 7 and 30 days post-IHKA induced status epilepticus (SE) to determine expression of GLT-1 and GLAST during epileptogenesis.

EXPERIMENTAL PROCEDURES

Animals

8–10-week-old Charles River CD1 male mice were housed under a 12-h light and 12-h dark cycle with *ad libitum* access to food and water. All experiments performed were approved by the University of California, Riverside Institutional Animal Care and Use Committee (IACUC) and were conducted in accordance with the National Institutes of Health (NIH) guidelines. A total of 53 mice were used in this study.

Kainic-acid induced status epilepticus

Intrahippocampal kainic acid (IHKA) injections were used to induce epileptogenesis as previously described (Lee et al., 2012; Hubbard et al., 2016). Mice were anesthetized with a solution of ketamine (80 mg/kg)/xylazine (10 mg/kg) and positioned in a stereotaxic frame. The skull was exposed, bregma was located, and a craniotomy was performed 1.8 mm posterior and 1.6 mm lateral to bregma. Mice were injected with either 64 nL of 0.9% saline or 20 mM kainic acid (Tocris) using a microinjector (Nanoject II, Drummond Scientific) into the CA1 region of the dorsal hippocampus (lowered to 1.9 mm dorsoventral). Following injections, mice experienced status epilepticus, defined by Racine scale stage 3–5 seizures (Racine, 1972) for at least 3 h. The presence of epileptiform activity and the development of spontaneous seizures has previously been confirmed by chronic video-EEG recordings to occur in 100% of animals after IHKA injections (Lee et al., 2012). We monitored mice for 5 h following IHKA injection using video recording to verify the presence of Racine stage 3–5 seizures. All animals included in this study experienced continuous status epilepticus (SE), characterized by forelimb and hindlimb clonus, rearing, jumping, and falling (Racine, 1972). Animals that died due to SE were excluded from the study. Mice were euthanized at 1, 3, 7, and 30 days (n = 9 for each time point) after IHKA-induced status epilepticus and 1 and 7 days (n = 17 total animals) after intrahippocampal saline injections.

Immunohistochemistry

Mice were euthanized with Fatal Plus (Western Medical Supply) then perfused with ice-cold phosphate buffered saline (PBS) followed by 4% paraformaldehyde (PFA). Brains were harvested and fixed in 4% PFA for two hours at 4 °C. Harvested brains were then transferred and stored in 30% sucrose at 4 °C until use. Prior to sectioning, harvested brains were flash frozen with isopentane. Frozen brains were sealed in optimum cutting temperature (O.C.T.) formulation at 20 °C and sliced into 50 μm sections using a cryostat (Leica CM 1950). Sections were stored in 0.01% sodium azide PBS at 4 °C. Slices were collected from each animal (IHKA n = 3 animals per time point, saline n = 5). For each animal, 8 sections were processed for immunohistochemistry, 4 ventral and 4 dorsal to the injection site. Sections were washed with PBS prior to immunohistochemistry. Endogenous peroxidase activity was quenched with 3% H_2O_2 at room temperature for 1 h and then washed once with PBS. Next, sections were blocked for 1 h at room temperature with 5% normal goat serum. Sections were then incubated overnight at 4 °C with primary antibodies to GLT-1 (1:3000, Abcam AB41621), GLAST (1:200, Abcam AB416) and glial fibrillary acidic protein (GFAP; 1:200, Millipore MAB360) in 0.3% Triton-X-100. The next day, sections were washed with PBS and incubated with HRP-conjugated secondary antibodies (HRP Goat Anti-Rabbit; 1:100, Molecular Probes/Invitrogen T20922) 30 min RT. Then, sections were washed with PBS and incubated with species-specific secondary antibodies conjugated with Alexa 488-tyramide or Alexa 594 (Molecular Probes/Invitrogen) for visualization. Sections were again washed before being mounted in Vectashield with DAPI (Vector Laboratories). To obtain overall hippocampal images for quantitation, imaging was done at 5 × using a fluorescence microscope (Leica DFC345FX) under identical settings for each channel.

Quantification was performed using ImageJ software. A large box representing the region of interest (ROI) was drawn to denote all layers of the hippocampus and individual boxes identifying individual layers were drawn on the DAPI channel at the center of each layer of the hippocampus: stratum (S.) oriens, S. pyramidale of CA1, S. radiatum, S. lacunosum moleculare (SLM), molecular layer, upper blade of the dentate gyrus, hilus, lower blade of the dentate gyrus, S. lucidum, and S. pyramidale of CA3.

Synaptosomal fractionation

Mice were euthanized with Fatal Plus (Western Medical Supply) and perfused with ice-cold PBS containing protease inhibitors (Roche). Dorsal hippocampus was microdissected ice-cold at 1, 3, 7 and 30 days post-IHKA or 1 and 7 days post-saline injection (n = 6 animals per IHKA time point; n = 12 animals for saline controls). An efficient protocol for crude synaptosomal fractionation (Fig. 1A) was carefully modified from

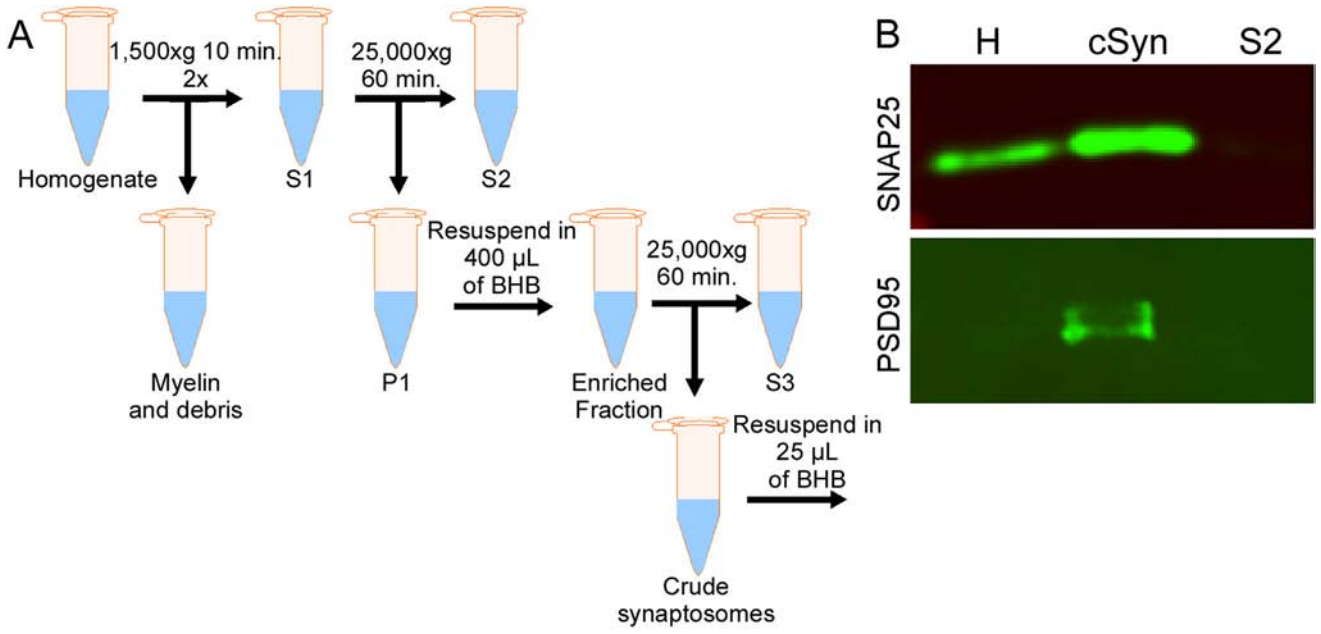

Fig. 1. Synaptosomal fractionation. A. Schematic of crude synaptosomal fractionation method used. B. Western blot of synaptosomal fractionation protein markers. Whole tissue homogenate (H), crude synaptosomal fractions (cSyn), and supernatant 2 (S2) were probed for postsynaptic density protein 95 (PSD95; ~95 KDa), and synaptosomal-associated protein 25 (SNAP25; ~25 KDa).

(Evans, 2015). Harvested tissue was stored in brain homogenization buffer (BHB; 320 mM sucrose, 1 mM EDTA, 5 mM Tris base, protease inhibitors (Roche), pH 7.4) and flash frozen at −80 °C until use. Tissue was suspended in 200 µL of BHB and homogenized using the Bullet Blender (Next Advance) at setting 8 for 4 min and setting 12 for 1 min at 4 °C. Next, samples were centrifuged at 1500 × *g* (3,992 rpm) for 10 min at 4 °C using the Eppendorf 5424R centrifuge. The supernatant was transferred to 10 mL thick-walled polypropylene tubes (Beckman Coulter). Pellets were resuspended in 200 µL of BHB, centrifuged again at 1500 × *g* for 10 min, and supernatants were pooled (S1). Supernatants were centrifuged at 25,000 × *g* for 60 min using the Allegra X-30R centrifuge (Beckman Coulter) with the F1010 rotor. Supernatant (S2) was saved and used to represent the non-synaptosomal cellular components. Pellet (P1) was washed and resuspended in 400 µL of BHB and centrifuged again at 25,000 × *g* for 60 min. The supernatant was discarded. The pellet containing the crude synaptosomal pellet was resuspended in 25 µL of BHB and prepared for Western blot analysis. Crude synaptosomal fractions were collected to ensure the inclusion of astrocytes found at the tripartite synapse. Total protein was quantified with a Bradford assay and crude synaptosomal fractionation was confirmed with synaptic markers for synaptosomal-associated protein 25 (SNAP25) and postsynaptic density protein 95 (PSD95) (Fig. 1B). The following antibodies were used: mouse anti-SNAP25 (1:1000; Abcam ab66066) and mouse anti-PSD95 (1:1000; Abcam ab2723).

Western blotting

Total protein concentrations of homogenized and fractionated tissue samples were obtained using a Bradford assay. Protein was resolved by sodium dodecyl sulfate polyacrylamide gel electrophoresis (SDS-PAGE) using 10% polyacrylamide gels and then transferred to a nitrocellulose membrane. Following transfer, nitrocellulose membranes were incubated in total protein stain (TPS) solution (REVERT™ Total Protein Stain) for normalization. Bands were visualized and quantified using the LI-COR Odyssey Fc Western Imaging System. Following total protein stain, membranes were briefly rinsed with water and blocked for 1 h in 5% milk in Tris-buffered saline 0.1% Tween 20 (Sigma) at room temperature (RT). Membranes containing IHKA and saline control samples were then probed for either GLT-1 (1:5000, Abcam ab41621) or GLAST (1:500, Abcam ab416). Bands were visualized and quantified using species specific antibodies (IRDye; LI-COR) and the LI-COR Odyssey Fc Western Imaging System. Protein levels were normalized to TPS as described by LI-COR in *REVERT™ Total Protein Stain Packet Insert.*

$$\text{Lane Normalization Factor} = \frac{\text{TPS for Each Lane}}{\text{TPS signal from the Lane with the Highest TPS signal}}$$

$$\text{Normalized Signal} = \frac{\text{Target Band Signal}}{\text{Lane Normalization Factor}}$$

Statistical analysis

Statistical analysis was performed using Prism 8 software (GraphPad Software, La Jolla, CA). All datasets were first tested for assumptions of normality and equality of variance. The Shapiro–Wilk (W) test was used to test for normal distribution and the Brown-Forsythe test was used to test for equal variance in our sample distribution. A one-way ANOVA with *post hoc* Bonferroni multiple comparisons tests

was used for samples that had normal distribution and equal variance. If either normal distribution and/or equal variance assumptions were not satisfied, a Kruskal-Wallis (H) non-parametric test was used with Dunn's multiple comparisons tests. All data points were depicted in figures for data analyzed using non-parametric tests. All error bars are presented as the mean ± standard error of the mean (SEM). Difference from saline control was considered statistically significant by a *P*-value <0.05, <0.01, <0.001 or <0.0001 and was denoted with one, two, three or four asterisks (*), respectively. Difference between treatments was quantified for Western blot analysis and was considered statistically significant by a *P*-value of <0.05 or <0.01 and was denoted with one or two asterisks (*), respectively. Saline controls were grouped after initial statistical analysis performed using an unpaired t-test showed no significant differences between 1- and 7-day saline-injected controls ($P > .05$).

RESULTS

We found a significant increase in GLT-1 immunoreactivity at 1 and 3 days post-IHKA in both hippocampi and a significant downregulation at 7 days post-IHKA in the ipsilateral hippocampus. GLT-1 synaptosomal protein levels were significantly decreased 7 days post-IHKA in the ipsilateral hippocampus. GLAST immunoreactivity was significantly increased at 1 day and 3 days post-IHKA in the ipsilateral hippocampus. GLAST synaptosomal protein levels were not significantly different from saline controls but there was a significant difference in ipsilateral GLAST synaptosomal levels between 7 days and 30 days post-IHKA in the ipsilateral hippocampus. These results indicate a significant change in glutamate transporter expression and localization during epileptogenesis.

Glutamate transporter-1 (GLT-1) expression in the dorsal hippocampus

Hippocampal GLT-1 and GFAP immunoreactivity were assessed at 1, 3, 7 and 30 days post-intrahippocampal kainic acid (IHKA) induced status epilepticus (SE) and for saline-injected animals (controls) for hippocampi both ipsilateral **(**Fig. 2**,** Fig. 3**)** and contralateral **(**Fig. 4**,** Fig. 5**)** to injection. We have previously demonstrated that GLT-1 immunoreactivity is altered and GFAP immunoreactivity is increased in the hippocampi following a higher dose kainic acid injection of 74 nL (Hubbard et al., 2016). For this study, we selected a lower dose kainic acid injection volume of 64 nL to decrease mortality. Characteristics of hippocampal sclerosis including dentate granule cell dispersion, neuronal loss in CA1, and gliosis were observed, and are all hallmark features of temporal lobe epilepsy (TLE) (Thom, 2014).

A one-way ANOVA on GLT-1 immunoreactivity in the ipsilateral total hippocampus post-IHKA revealed a main effect of time point ($F(4,12) = 38.96$, $P < .0001$) **(**Fig. 3**)**. *Post hoc* Bonferroni tests revealed a significant increase in GLT-1 immunoreactivity at 1 ($P < .0001$) and 3 days post-IHKA ($P < .0001$), followed by a downregulation at 7 days post-IHKA ($P = .0223$), and this returned to near baseline levels by 30 days post-IHKA in the ipsilateral hippocampus ($P > .05$) compared to saline controls **(**Fig. 3**)**. To determine localized differences within the hippocampus, one-way ANOVAs for each region on GLT-1 immunoreactivity revealed a main effect of time point in *S. oriens* ($F(4,12) = 8.032$, $P = .0022$), S. pyramidale ($F(4, 12) = 10.81$, $P = .0006$), SLM ($F(4,12) = 27.92$, $P < .0001$), molecular layer ($F(4,12) = 29.86$, $P < .0001$), the upper blade of the dentate gyrus ($F(4,12) = 44.84$), $P < .0001$), hilus ($F(4,12) = 6.585$, $P = .0048$), lower blade of the dentate gyrus ($F(4,12) = 5.775$, $P = .0079$), and *S. lucidum* ($F(4,12) = 11.70$, $P = .0004$) in the ipsilateral hippocampus post-IHKA. At 1 day post-IHKA, *post hoc* Bonferroni tests revealed that GLT-1 immunoreactivity was significantly increased in S. pyramidale of CA1 ($P = .0045$), SLM ($P < .0001$), the upper blade of the dentate gyrus ($P < .0001$) and *S. lucidum* ($P = .0020$). At 3 days post-IHKA, GLT-1 immunoreactivity was significantly increased in *S. oriens* ($P = .0049$), S. pyramidale of CA1 ($P = .0027$), SLM ($P < .0001$), and the molecular layer ($P < .0001$). *Post hoc* Bonferroni tests revealed at 7 days post-IHKA, overall GLT-1 immunoreactivity is significantly decreased in the ipsilateral hippocampus ($P = .0196$). Specifically, at 7 days post-IHKA, GLT-1 immunoreactivity was decreased in the upper ($P = .0158$) and lower blade of the dentate gyrus ($P = .0196$). At 30 days post-IHKA, there were no significant differences in GLT-1 immunoreactivity between saline and IHKA injected mice ($P > .05$). Overall, there was an upregulation in GLT-1 immunoreactivity at early time points following status epilepticus and a downregulation of GLT-1 immunoreactivity at 7 days post-IHKA that returned to baseline levels by 30 days post-IHKA in the ipsilateral hippocampus.

GLT-1 immunoreactivity was also assessed in the contralateral hippocampus following intrahippocampal kainic acid (IHKA) induced status epilepticus (SE) and for saline injected animals (controls) **(**Fig. 4**,** Fig. 5**)**. A one-way ANOVA on GLT-1 immunoreactivity in the contralateral total hippocampus post-IHKA revealed no main effect on time point ($F(4,12) = 1.810$, $P > .05$) **(**Fig. 5**)**. Interestingly, a one-way ANOVA revealed a main effect of time on GLT-1 immunoreactivity in *S. oriens* ($F(4,12) = 9.138$, $P = .0013$), SLM ($F(4,12) = 5.666$, $P = .0085$), molecular layer ($F(4,12) = 3.262$), $P = .0499$), and the hilus ($F(4,12) = 3.264$, $P = .0498$) in the contralateral hippocampus post-IHKA. *Post hoc* Bonferroni tests revealed at 1 day post-IHKA, GLT-1 immunoreactivity was increased in SLM ($P = .0033$), molecular layer ($P = .0229$) and hilus ($P = .0213$). At 3 days post-IHKA, GLT-1 immunoreactivity was increased in *S. oriens* ($P = .001$). There were no observed changes in GLT-1 immunoreactivity at 7 and 30 days post-IHKA in the contralateral hippocampus when compared to saline-injected animals ($P > .05$). Overall, changes in GLT-1 immunoreactivity during epileptogenesis in both the ipsilateral and contralateral hippocampus were observed mainly in the dentate gyrus and primary astrocytic layers: SLM, *S. radiatum*, and molecular layer.

Synaptosomal expression of glutamate transporter-1 (GLT-1)

We isolated synaptosomes to ensure collection of all three elements of the tripartite synapse: pre-synaptic terminals,

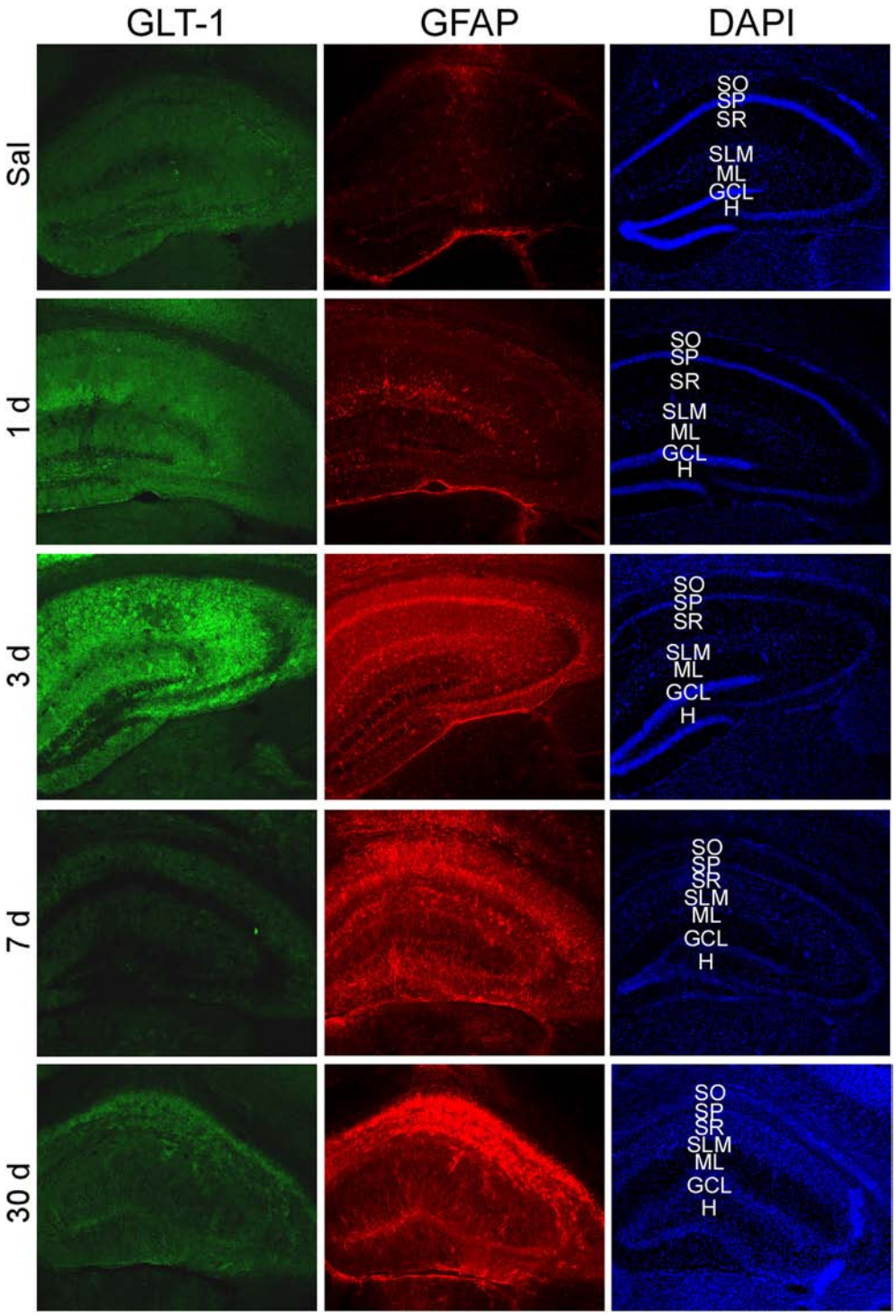

Fig. 2. Glutamate transporter-1 (GLT-1) and glial fibrillary acidic protein (GFAP) immunoreactivity in the ipsilateral dorsal hippocampus after kainic acid-induced status epilepticus. 5 × images of GLT-1 (green), GFAP (red), and DAPI (blue) immunoreactivity in the ipsilateral dorsal hippocampus after saline injections (control) and 1, 3, 7 and 30 days post-SE. SO = stratum oriens; SP = stratum pyramidale; SR = stratum radiatum; SLM = stratum lacunosum moleculare; ML = molecular layer; GCL = granule cell layer; H = hilus. (For interpretation of the references to color in this figure legend, the reader is referred to the web version of this article.)

post-synaptic elements, and perisynaptic astrocyte processes. Success of synaptosomal fractionation was confirmed by probing for synaptosomal markers (Fig. 1B). We specifically probed for SNAP25 and PSD95. SNAP25 is a presynaptic protein and a component of the SNARE-complex that is involved in vesicle membrane docking and fusion (Rizo and Sudhof, 2002). PSD95 is a postsynaptic protein that is involved in anchoring synaptic proteins (Sheng and Sala, 2001). SNAP25 and PSD95 were present in whole tissue homogenates and markedly elevated in the enriched synaptosomal fractions (Fig. 1B). Supernatant 2 (S2) containing the non-synaptosomal components did not contain traces of SNAP25 or PSD95, further confirming a successful fractionation (Fig. 1B).

We have previously discovered differences in total GLT-1 expression in the dorsal hippocampus during epileptogenesis (Hubbard et al., 2016). To improve our understanding of GLT-1 regulation in the IHKA model of epilepsy, we examined synaptosomal regulation of this transporter during epileptogenesis for the first time. A one-way ANOVA on GLT-1 synaptosomal protein levels in the ipsilateral hippocampus post-IHKA revealed a main effect of time point ($F(4, 31) = 5.706$, $P = .0015$) (Fig. 6). Specifically, pairwise *post hoc* Bonferroni tests revealed a significant down-regulation in synaptosomal GLT-1 expression at 7 days post-IHKA ($P = .0064$) that returned to near baseline levels by 30 days post-IHKA in the ipsilateral hippocampus ($P > .05$) (Fig. 6C). Interestingly, we did not observe a change in synaptosomal GLT-1 expression at 1 or 3 days post-IHKA (all $P > .05$) (Fig. 6C). There was also a significant difference in synaptosomal GLT-1 expression between 7 days post-IHKA and 30 days post-IHKA in the ipsilateral hippocampus ($P = .0023$) (Fig. 6C).

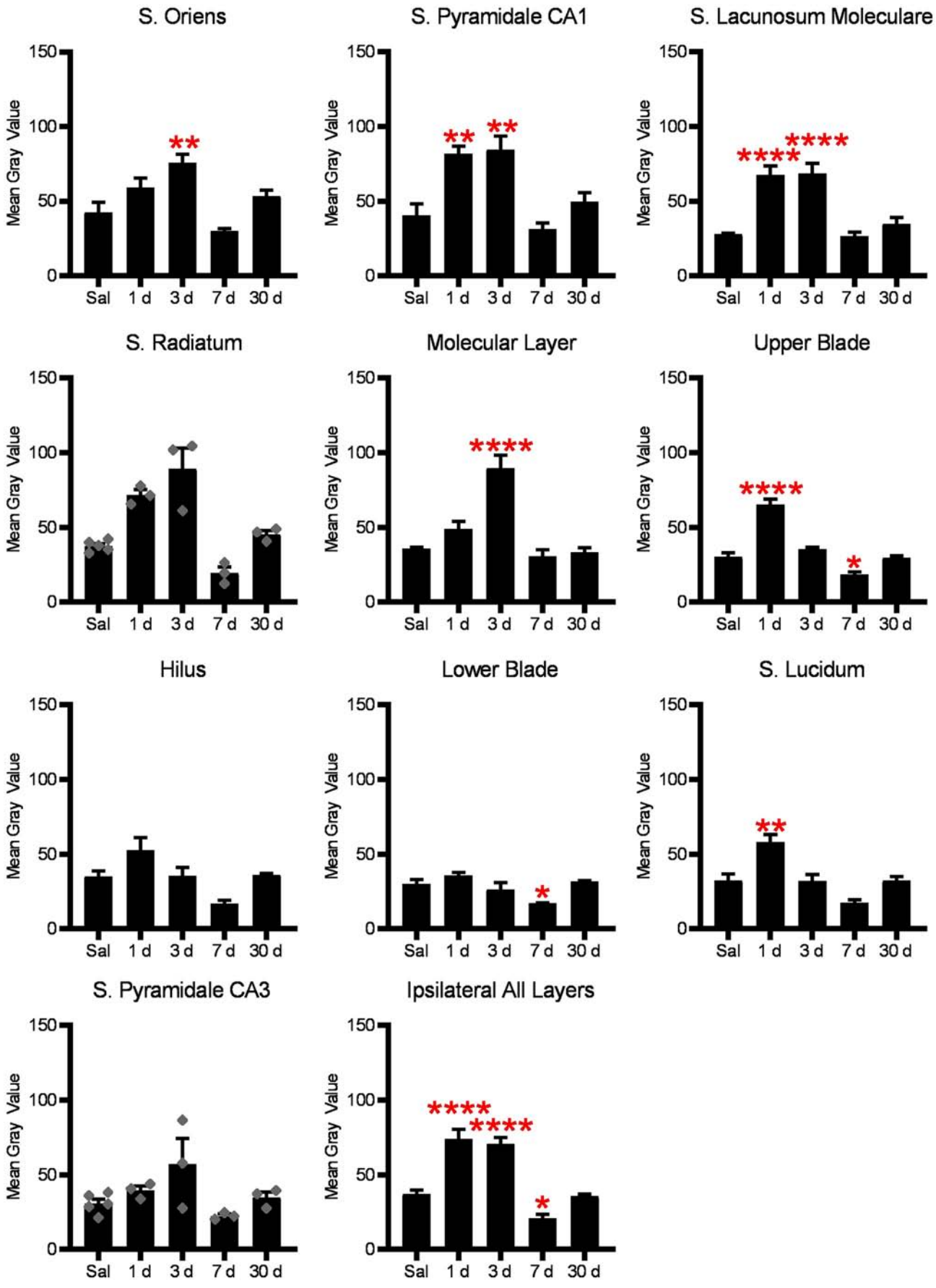
S. Oriens
S. Pyramidale CA1
S. Lacunosum Moleculare
S. Radiatum
Molecular Layer
Upper Blade
Hilus
Lower Blade
S. Lucidum
S. Pyramidale CA3
Ipsilateral All Layers
Mean Gray Value
150
100
50
0
Sal
1 d
3 d
7 d
30 d
**
**
**
****
****
****
*
*
**
****
****
*

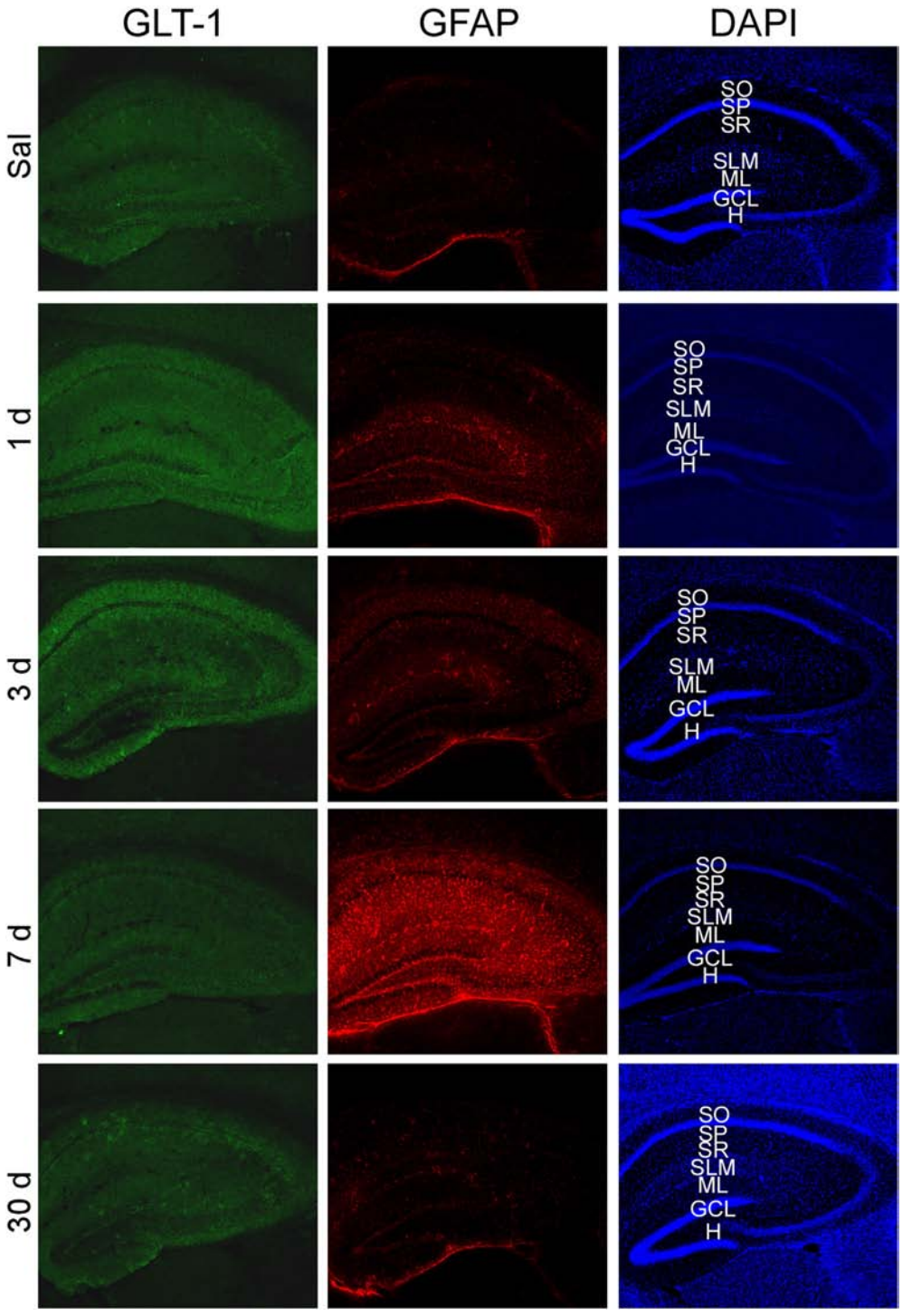

Fig. 4. Glutamate transporter-1 (GLT-1) and glial fibrillary acidic protein (GFAP) immunoreactivity in the contralateral dorsal hippocampus after kainic acid-induced status epilepticus. 5 × images of GLT-1 (green), GFAP (red), and DAPI (blue) immunoreactivity in the contralateral dorsal hippocampus after saline injections (control) and 1, 3, 7 and 30 days post-SE. SO = stratum oriens; SP = stratum pyramidale; SR = stratum radiatum; SLM = stratum lacunosum moleculare; ML = molecular layer; GCL = granule cell layer; H = hilus. (For interpretation of the references to color in this figure legend, the reader is referred to the web version of this article.)

While no changes in synaptosomal GLT-1 protein levels were observed at 1 or 3 days post-IHKA we did observe changes in GLT-1 immunoreactivity at these early time points, suggesting that overall but *not* synaptic GLT-1 protein levels may be upregulated early after KA-induced SE. There were no changes observed in synaptosomal GLT-1 expression in the contralateral dorsal hippocampus during epileptogenesis ($P > .05$) **(**Fig. 6F**)**.

Glutamate aspartate transporter (GLAST) expression in the dorsal hippocampus

Hippocampal GLAST immunoreactivity was assessed after 1, 3, 7 and 30 days post-intrahippocampal kainic acid (IHKA) induced status epilepticus (SE) and for saline-injected animals (controls) for hippocampi both ipsilateral **(**Fig. 7**,** Fig. 8**)** and contralateral **(**Fig. 9**,** Fig. 10**)** to injection.

A one-way ANOVA on GLAST immunoreactivity in the ipsilateral total hippocampus post-IHKA revealed no main effect of time ($F(4,12) = 2.235$, $P > .05$) **(**Fig. 8**)**. Interestingly, a one-way ANOVA revealed a main effect of time on GLAST immunoreactivity in *S. oriens* ($F(4,12) = 3.474$, $P = .0418$), S. pyramidale of CA1 ($F(4,12) = 7.512$), $P = .0029$), *S. radiatum* ($F(4,12) = 24.11$, $P < .0001$), SLM ($F(4,12) = 13.85$), $P = .0002$), molecular layer ($F(4, 12) = 19.90$, $P < .0001$), upper blade ($F(4,12) = 8.551$, $P = .0017$), hilus (F

Fig. 3. Quantification of glutamate transporter-1 (GLT-1) immunoreactivity in the ipsilateral dorsal hippocampus. Mean gray scale values shown at the indicated time points after kainic acid-induced status epilepticus. For each time point post-IHKA, n = 3 animals were used. For saline injections (controls), n = 5 animals were used. * indicates $P < .05$, ** indicates $P < .01$, *** indicates $P < .001$ and **** indicates $P < .0001$ when compared to saline-injected animals (control).

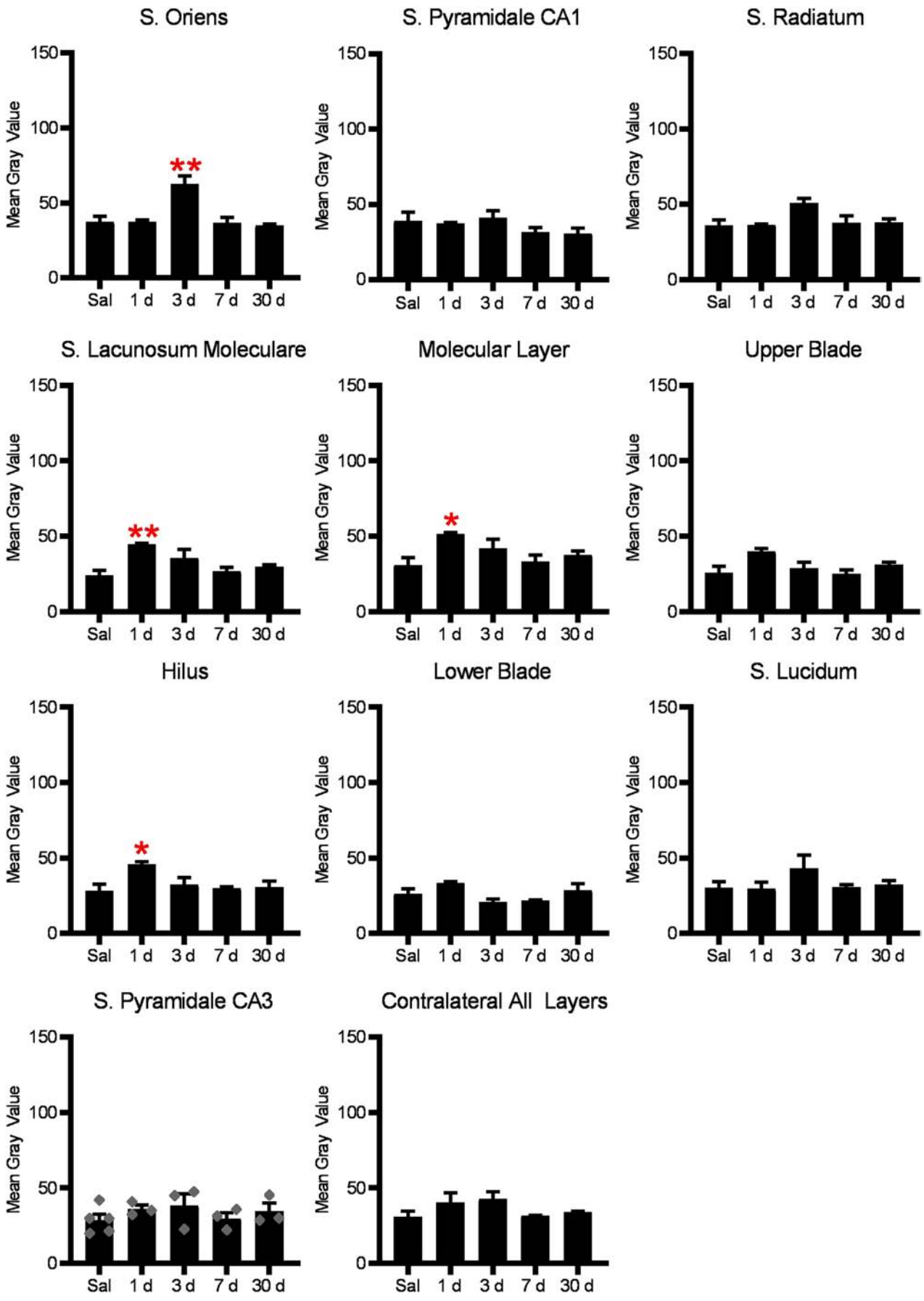
S. Oriens
S. Pyramidale CA1
S. Radiatum
S. Lacunosum Moleculare
Molecular Layer
Upper Blade
Hilus
Lower Blade
S. Lucidum
S. Pyramidale CA3
Contralateral All Layers
Mean Gray Value
150
100
50
0
Sal
1 d
3 d
7 d
30 d
**
*

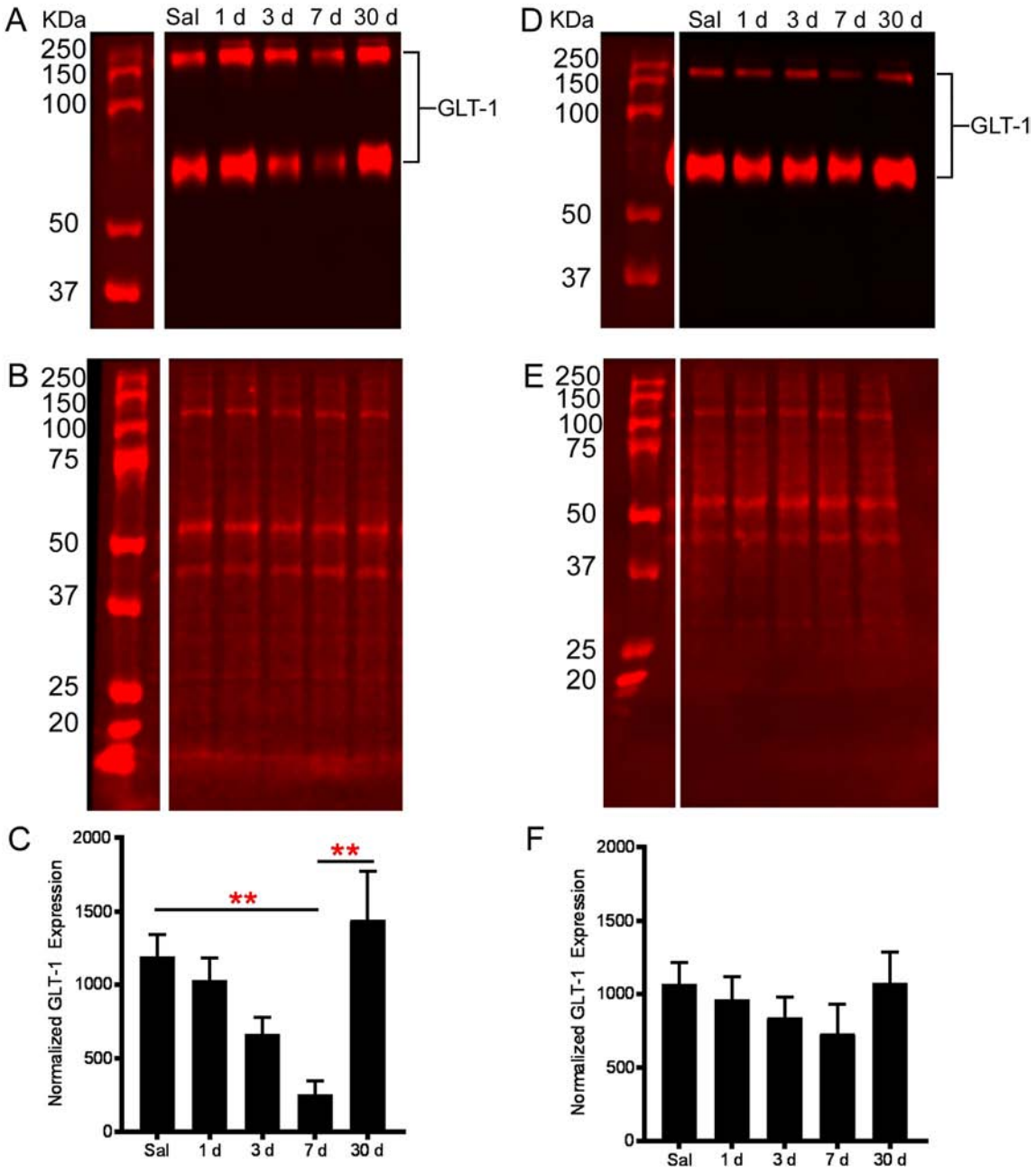

Fig. 6. Synaptosomal glutamate transporter-1 (GLT-1) expression in the IHKA model of epilepsy. A. Representative Western blot of GLT-1 in saline controls and 1, 3, 7 and 30 days post-SE in the ipsilateral dorsal hippocampus. B. Total protein stain indicating equivalent protein loading (1 μg) for ipsilateral dorsal hippocampus. C. Quantification of GLT-1 band intensities at each time point normalized to total protein stain in the ipsilateral dorsal hippocampus. D. Representative Western blot of GLT-1 in saline controls and 1, 3, 7, and 30 days post-SE in the contralateral dorsal hippocampus. E. Total protein stain indicating equivalent protein loading (1 μg) for contralateral dorsal hippocampus. F. Quantification of GLT-1 band intensities at each time point normalized to total protein stain in the contralateral dorsal hippocampus. For each time point post-IHKA, n = 6 animals were used. For saline-injected (control), n = 12 animals were used. ** indicates $P < .01$.

(4,12) = 18.43, $P < .0001$) and lower blade (F(4,12) = 29.56, $P < .0001$) of the dentate gyrus, *S. lucidum* (F (4,12) = 7.025, $P = .0037$), and S. pyramidale of CA3 (F (4,12) = 8.697, $P = .0016$). *Post hoc* Bonferroni tests revealed at 1 day post-IHKA, GLAST immunoreactivity was significantly increased in S. pyramidale of CA1 ($P = .0040$), *S. radiatum* ($P < .0001$), SLM ($P = .0001$), molecular layer ($P < .0001$), the upper blade ($P = .0019$) and lower blade ($P < .0001$) of the dentate gyrus, *S. lucidum* ($P = .0203$), and S. pyramidale of CA3 ($P = .0034$). At 3 days

Fig. 5. Quantification of glutamate transporter-1 (GLT-1) immunoreactivity in the contralateral dorsal hippocampus. Mean gray scale values shown at the indicated time points after kainic acid-induced status epilepticus. For each time point post-IHKA, n = 3 animals were used. For saline injections (controls), were used. * indicates $P < .05$ and ** indicates $P < .01$ when compared to saline-injected animals (control).

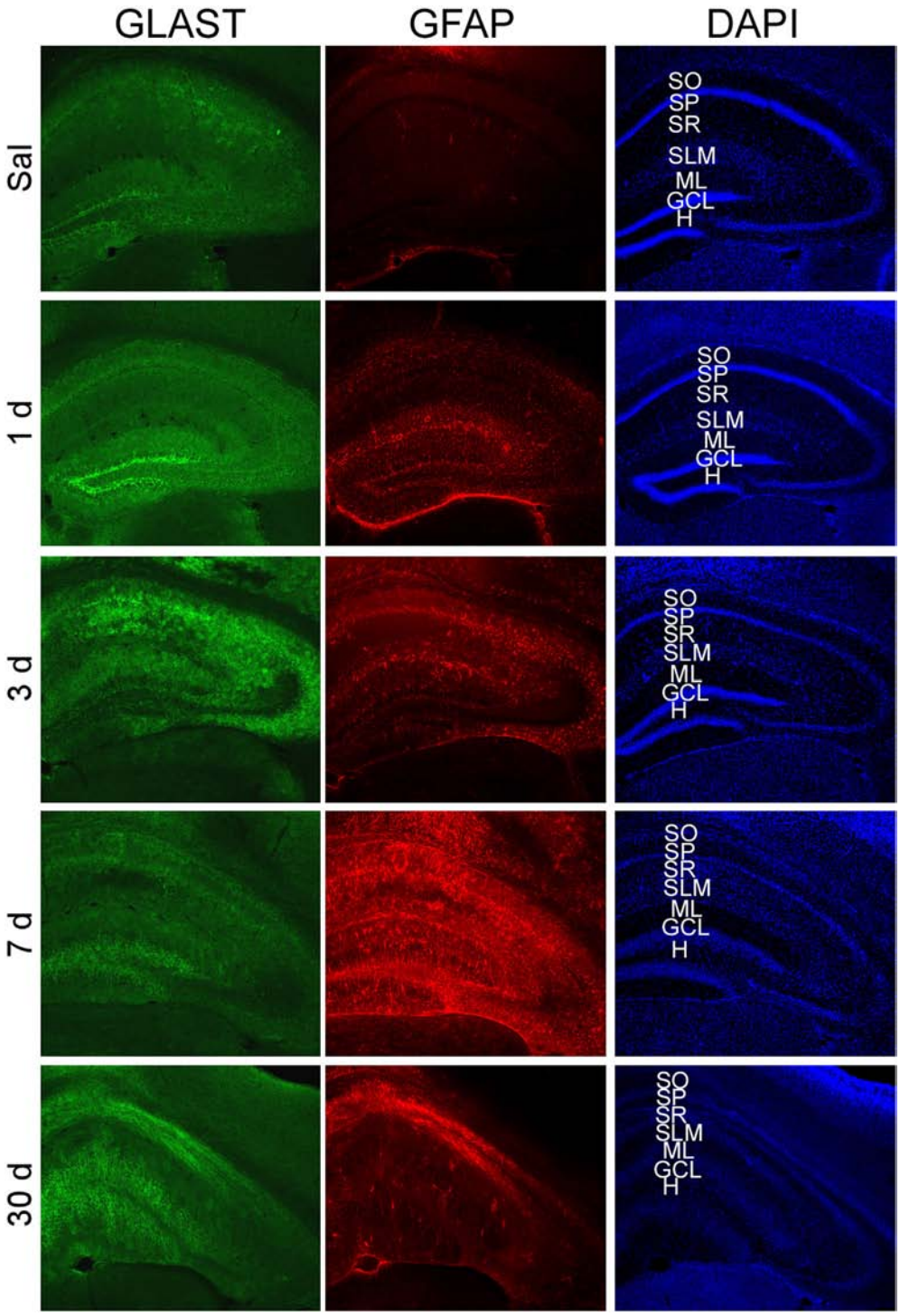

Fig. 7. Glutamate aspartate transporter (GLAST) and glial fibrillary acidic protein (GFAP) immunoreactivity in the ipsilateral dorsal hippocampus after kainic acid-induced status epilepticus. 5× images of GLAST (green), GFAP (red), and DAPI (blue) immunoreactivity in the ipsilateral dorsal hippocampus after saline injections (control) and 1, 3, 7 and 30 days post-SE. SO = stratum oriens; SP = stratum pyramidale; SR = stratum radiatum; SLM = stratum lacunosum moleculare; ML = molecular layer; GCL = granule cell layer; H = hilus. (For interpretation of the references to color in this figure legend, the reader is referred to the web version of this article.)

post-IHKA, GLAST immunoreactivity was significantly increased in S. pyramidale of CA1 (P = .0357), *S. radiatum* (P = .0003), and SLM (P = .0218). At 30 days post-IHKA, there was a significant increase in GLAST immunoreactivity from baseline in the primary astrocytic layer *S. radiatum* (P = .0054).

A one-way ANOVA revealed no main effect of time point on GLAST immunoreactivity in the contralateral total hippocampus post-IHKA ($F(4,12) = 0.5788$, $P > .05$) (Fig. 10).

Synaptosomal expression of glutamate aspartate transporter (GLAST)

We also aimed to determine GLAST synaptosomal expression during epileptogenesis. A Kruskal-Wallis non-parametric test revealed a main effect of time point on GLAST synaptosomal protein levels in the ipsilateral hippocampus post-IHKA ($H(5, 36) = 15.35$, P = .004). There were no significant changes in synaptosomal GLAST expression at 1, 3, 7 or 30 days post-IHKA compared to saline injected animals (controls) in the ipsilateral or contralateral dorsal hippocampus (Fig. 11). Interestingly, *post hoc* tests showed a significant upregulation in synaptosomal GLAST expression at 30 days post-IHKA compared with 7 days post-IHKA in the ipsilateral dorsal hippocampus (P = .033) (Fig. 11C) but not contralaterally ($P > .05$) (Fig. 11F).

DISCUSSION

In this study, we used immunohistochemistry, synaptosomal fractionation and Western blot analysis to examine changes in the Na^+-dependent glutamate transporters GLT-1 and GLAST at various time points post-IHKA induced status epilepticus in a mouse model of temporal lobe epilepsy. This is the first paper to directly assess levels of glutamate transporters at the synapse quantitatively during epileptogenesis. First, we found a significant upregulation in GLT-

1 immunoreactivity at 1 and 3 days post-IHKA in the dorsal hippocampus. Second, we found that GLT-1 immunoreactivity is significantly downregulated at 7 days post-IHKA in the ipsilateral hippocampus. Third, we found that synaptosomal GLT-1 protein levels were significantly downregulated 7 days post-IHKA in the ipsilateral hippocampus. Fourth, GLAST immunoreactivity was significantly increased at 1 day and 3 days post-IHKA in a layer-specific manner in the ipsilateral hippocampus. While the current study does not establish causation or mechanism, these results further support the hypothesis that astrocytic glutamate transporter dysregulation may contribute to the development of epilepsy.

Changes in glutamate transporter-1 (GLT-1) regional and cellular expression following SE

Numerous studies have established that there is an increase in extracellular glutamate levels during seizures (During and Spencer, 1993; Hubbard et al., 2013; Medina-Ceja et al., 2015; Soukupova et al., 2015). Increased levels of extracellular glutamate are likely due to excess glutamate release or reduced glutamate reuptake. GLT-1 is responsible for over 90% of the total glutamate clearance in the CNS (Danbolt, 2001). Therefore, changes in GLT-1 expression can greatly impact synaptic activity and function. Mice that globally lack GLT-1 develop lethal spontaneous epileptic seizures resulting in death early postnatally (Tanaka et al., 1997). Interestingly, mice that regionally lack GLT-1 only in the dorsal forebrain survive to adulthood but display transient focal seizures distinct from the generalized seizures observed in global GLT-1 knockout mice (Sugimoto et al., 2018). This study showed that regional loss of GLT-1 is sufficient to induce spontaneous seizures. Our current study is the first to examine changes in synaptosomal GLT-1 expression at both early and chronic time points during epileptogenesis. Our data are the first to address the subcellular pool of GLT-1 available for use at astrocytic perisynaptic processes, the functional site of glutamate uptake at glutamatergic synapses. Future studies will need to address the exact timing of onset of spontaneous seizures compared to timing of GLT-1 downregulation, and to determine whether manipulation of GLT-1 levels will inhibit epileptogenesis.

Excess extracellular glutamate has been shown to produce excitotoxicity in other neurological diseases including Alzheimer's disease (AD) and amyotrophic lateral sclerosis (ALS) (Foran and Trotti, 2009; Danysz and Parsons, 2012). GLT-1 expression and subcellular localization has also been shown to be altered in neurological diseases (Lin et al., 1998; Jacob et al., 2007; Foran et al., 2014; Munoz-Ballester et al., 2016; Zhang et al., 2017). Under normal physiological conditions, GLT-1 tends to cluster at astrocytic processes and endfeet and is localized at the plasma membrane (Schreiner et al., 2014). Recent studies have shown that GLT-1 dysfunction and changes in localization could be regulated at the post-translational level in many of these diseases (Huang et al., 2010; Foran et al., 2014; Zhang et al., 2017).

We found that GLT-1 protein levels change not only at the level of total protein expression in the dorsal hippocampus, using immunohistochemistry, but also change quantitatively at the subcellular level, using synaptosomal fractionation and Western blot analysis. We had previously determined with a higher-dose intrahippocampal kainic acid administration using immunohistochemistry that GLT-1 expression is upregulated at 1 day post-IHKA and downregulated by 4 days post-IHKA in the ipsilateral hippocampus (Hubbard et al., 2016). In the current study, we determined that GLT-1 expression is still upregulated at 3 days post-IHKA; therefore, there could be a major shift in GLT-1 levels between 3 and 4 days post-IHKA. We hypothesize that GLT-1 protein expression is upregulated as a compensatory response to the large amount of glutamate released during status epilepticus. For reasons that remain unclear, GLT-1 levels only remain upregulated for several days and subsequently decline significantly below baseline levels coinciding with the onset of spontaneous seizures in this model (Raedt et al., 2009). Synaptosomal GLT-1 protein is significantly downregulated 7 days post-IHKA in the ipsilateral hippocampus, indicating a reduction in perisynaptic GLT-1 levels available for glutamate uptake at the synapse. Interestingly, this observed downregulation in GLT-1 synaptosomal expression at 7 days post-IHKA corresponds well with the onset timing of spontaneous seizures in this model (about 7 days post-IHKA) which supports the possibility that downregulation of GLT-1 in perisynaptic astrocyte processes may precede and contribute to the onset of spontaneous seizures. Identification of changes in synaptosomal proteins provides us with valuable information on how synaptic function can change during disease progression (Valencia et al., 2013; Postupna et al., 2014; Lepeta et al., 2016). If there is less GLT-1 functioning at the tripartite synapse, and GLT-1 is responsible for the majority of glutamate clearance, we can infer there will likely be impaired glutamate uptake from the extracellular space. Elevated extracellular glutamate levels can induce seizures and *vice versa* which together contribute to the excitotoxic damage resulting in hippocampal sclerosis associated with TLE (Thom, 2014; Barker-Haliski and White, 2015).

Further studies will need to determine the molecular mechanisms responsible for GLT-1 protein downregulation in epileptogenesis. Understanding the mechanisms of downregulation of GLT-1 at day 7 could lead to an even more targeted, mechanistic way to prevent the onset of spontaneous seizures in this model. We previously determined that there are no significant changes in GLT-1 mRNA in the IHKA model of epilepsy, suggesting that regulation of GLT-1 occurs at the post-translational level (Hubbard et al., 2016). Future studies could examine potential post-translational modifications and mechanisms which have been determined to affect GLT-1 expression and function in other models of neurological disease such as sumoylation, Nedd4–2 trafficking, and palmitoylation (Huang et al., 2010; Foran et al., 2014; Zhang et al., 2017). EAAT2, the human analogue of GLT-1, is significantly decreased in patients with TLE (Proper et al., 2002); therefore, preventing this downregulation could be a potential antiepileptogenic

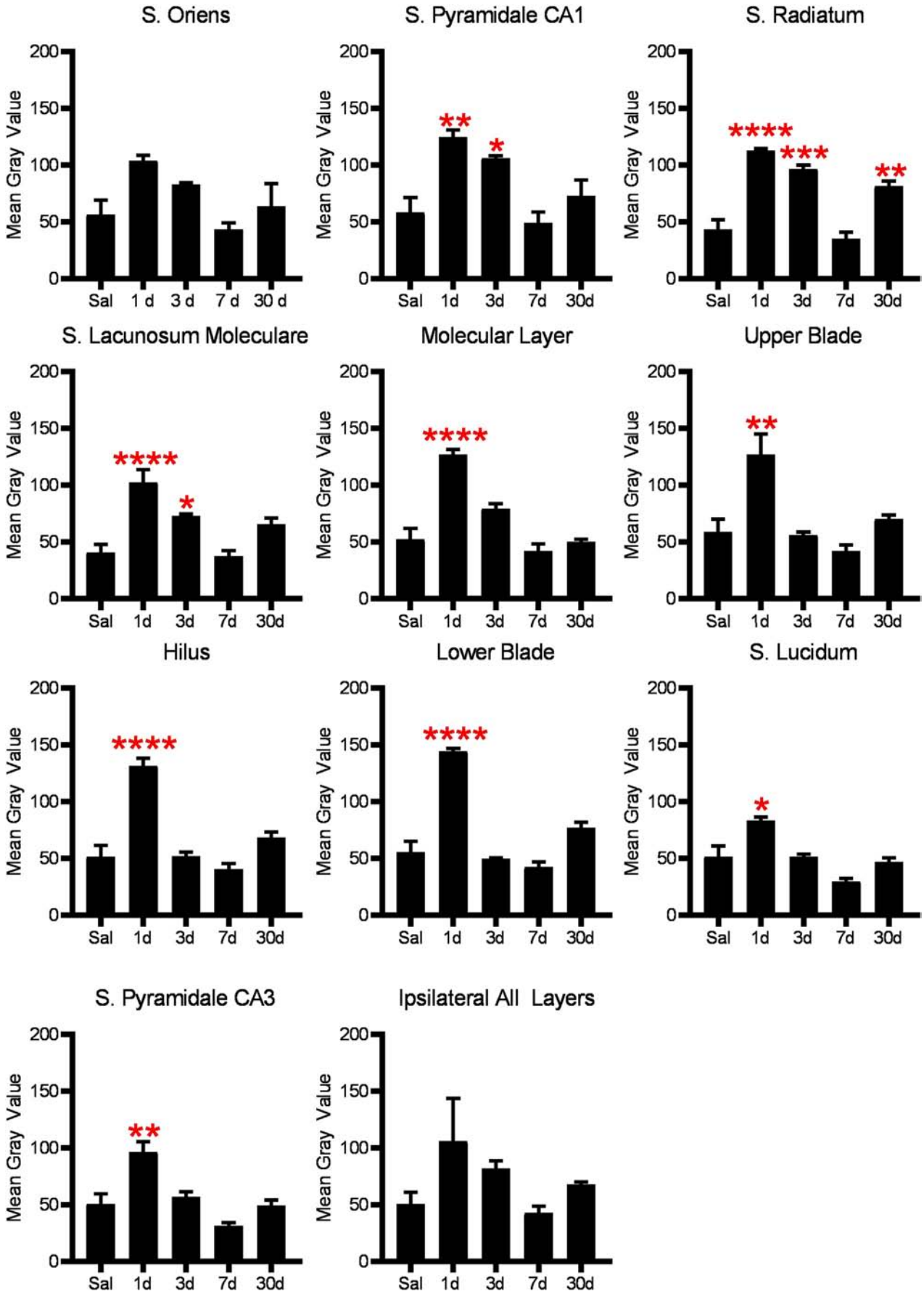
S. Oriens
S. Pyramidale CA1
S. Radiatum
S. Lacunosum Moleculare
Molecular Layer
Upper Blade
Hilus
Lower Blade
S. Lucidum
S. Pyramidale CA3
Ipsilateral All Layers
Mean Gray Value
0
50
100
150
200
Sal
1 d
3 d
7 d
30 d
1d
3d
7d
30d
*
**
***
****

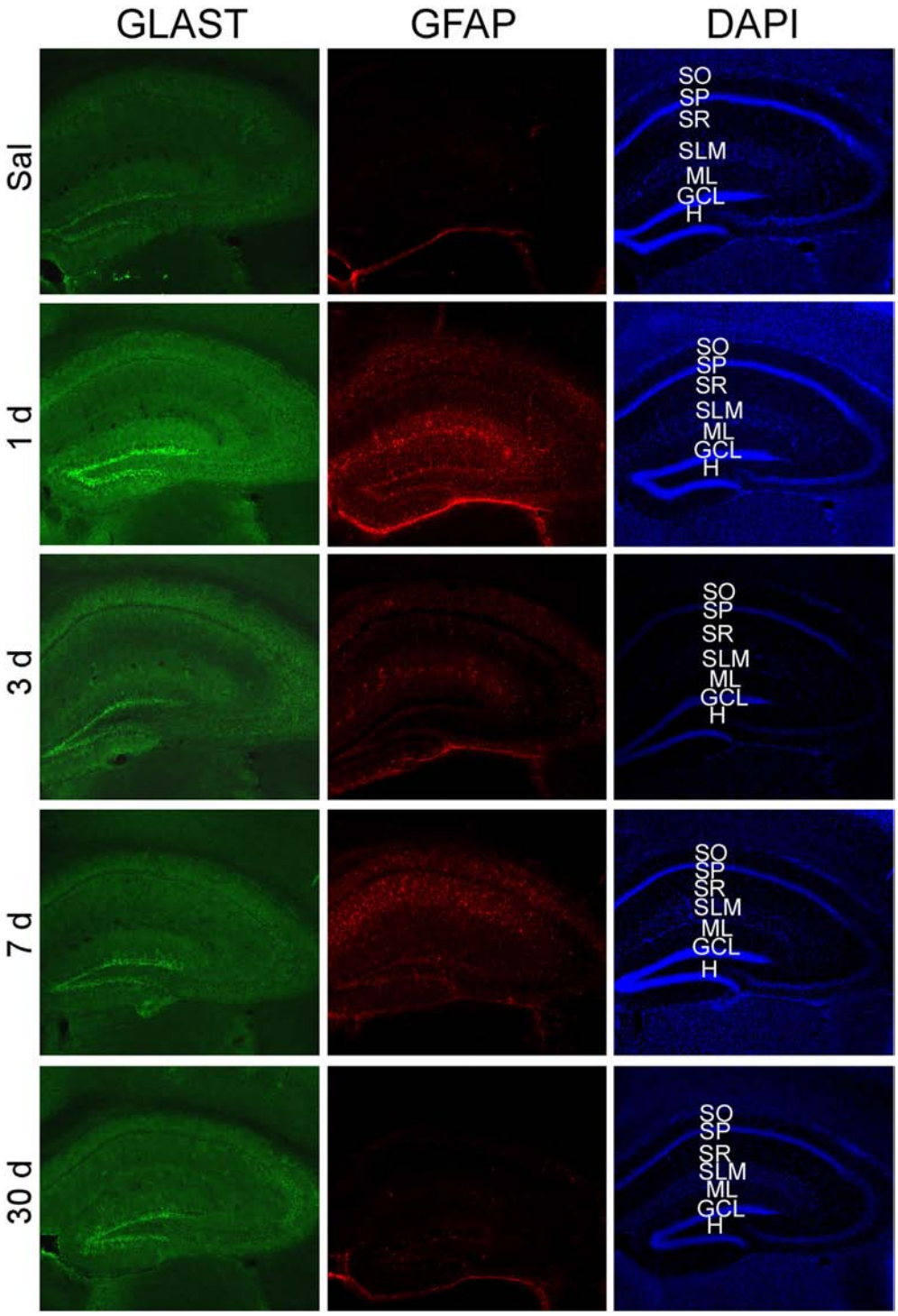

Fig. 9. Glutamate aspartate transporter (GLAST) and glial fibrillary protein (GFAP) immunoreactivity in the contralateral dorsal hippocampus after kainic acid-induced status epilepticus. 5× images of GLAST (green), GFAP (red), and DAPI (blue) immunoreactivity in the contralateral dorsal hippocampus after saline injections (control) and 1, 3, 7 and 30 days post-SE. SO = stratum oriens; SP = stratum pyramidale; SR = stratum radiatum; SLM = stratum lacunosum moleculare; ML = molecular layer; GCL = granule cell layer; H = hilus. (For interpretation of the references to color in this figure legend, the reader is referred to the web version of this article.)

and/or anticonvulsant strategy for patients with pharmacoresistant TLE. The generality of GLT-1 dysregulation in other forms of epilepsy also warrants further study.

Changes in glutamate aspartate transporter (GLAST) regional and cellular expression following SE

Changes in the human analogue of GLAST, EAAT1, have been observed in postmortem tissue of patients with temporal lobe epilepsy (Tessler et al., 1999). We found that there was an increase in hippocampal GLAST immunoreactivity at 1 and 3 days post-IHKA in the ipsilateral hippocampus. The increase in GLAST immunoreactivity paralleled the increase in GLT-1 immunoreactivity we observed at early time points following status epilepticus. However, synaptosomal GLAST protein levels were not significantly different from saline-injected control mice at early time points post-IHKA therefore their contribution to epileptogenesis in this model may not be as significant as GLT-1 dysregulation. Interestingly, we did observe a significant increase in synaptosomal GLAST levels at 30 days post-IHKA compared to 7 days post-IHKA in the ipsilateral hippocampus, a time when the hippocampus is sclerotic. This could potentially serve a compensatory function to increase astrocytic glutamate uptake in chronic hippocampal sclerosis.

Fig. 8. Quantification of glutamate aspartate transporter (GLAST) immunoreactivity in the ipsilateral dorsal hippocampus. Mean gray scale values shown at the indicated time points after kainic acid-induced status epilepticus. For each time point post-IHKA, n = 3 animals were used. For saline injections (controls), n = 5 animals were used. * indicates $P < .05$, ** indicates $P < .01$, *** indicates $P < .001$ and **** indicates $P < .0001$ when compared to

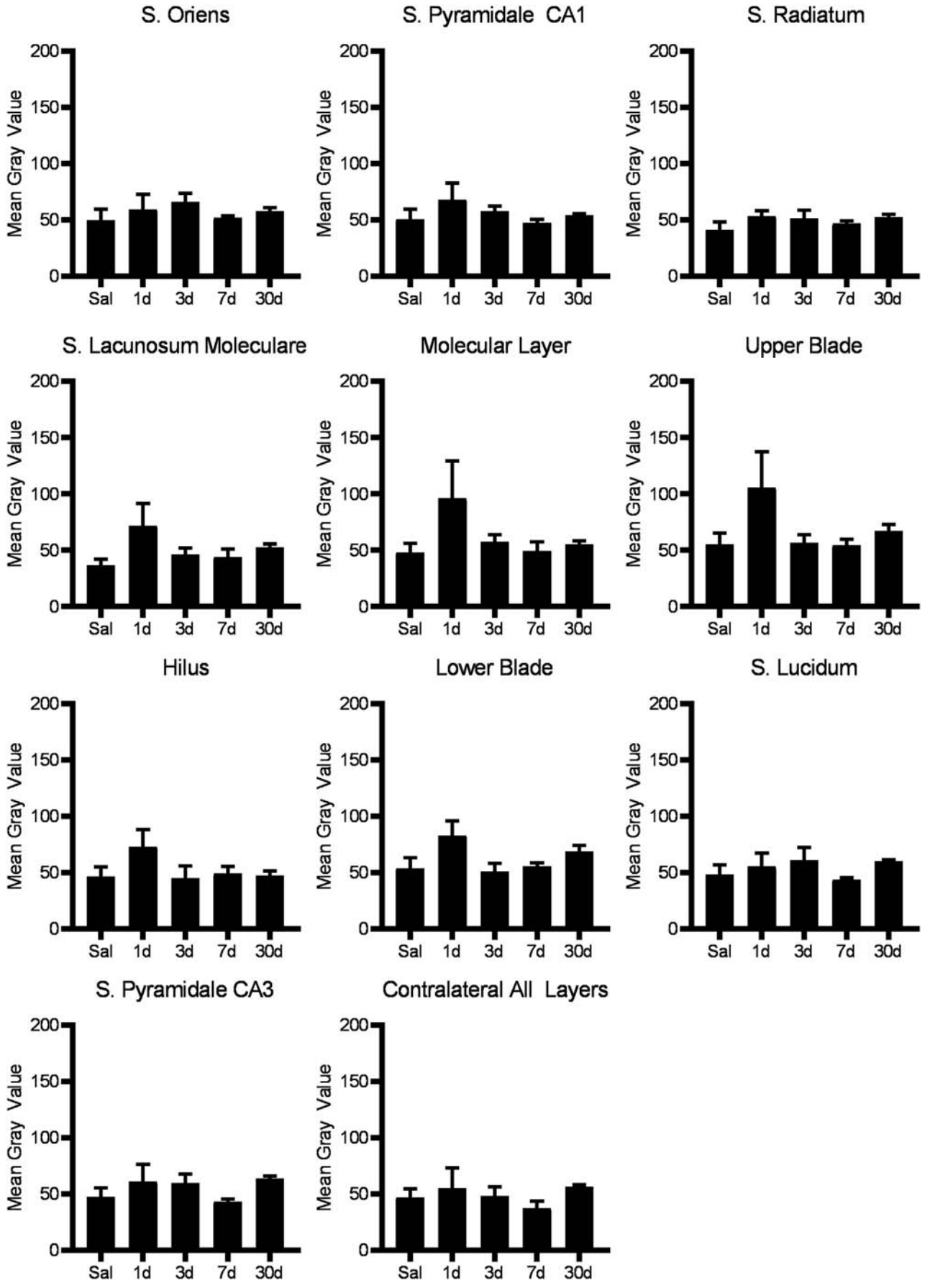
S. Oriens
S. Pyramidale CA1
S. Radiatum
S. Lacunosum Moleculare
Molecular Layer
Upper Blade
Hilus
Lower Blade
S. Lucidum
S. Pyramidale CA3
Contralateral All Layers
Mean Gray Value
0
50
100
150
200
Sal
1d
3d
7d
30d

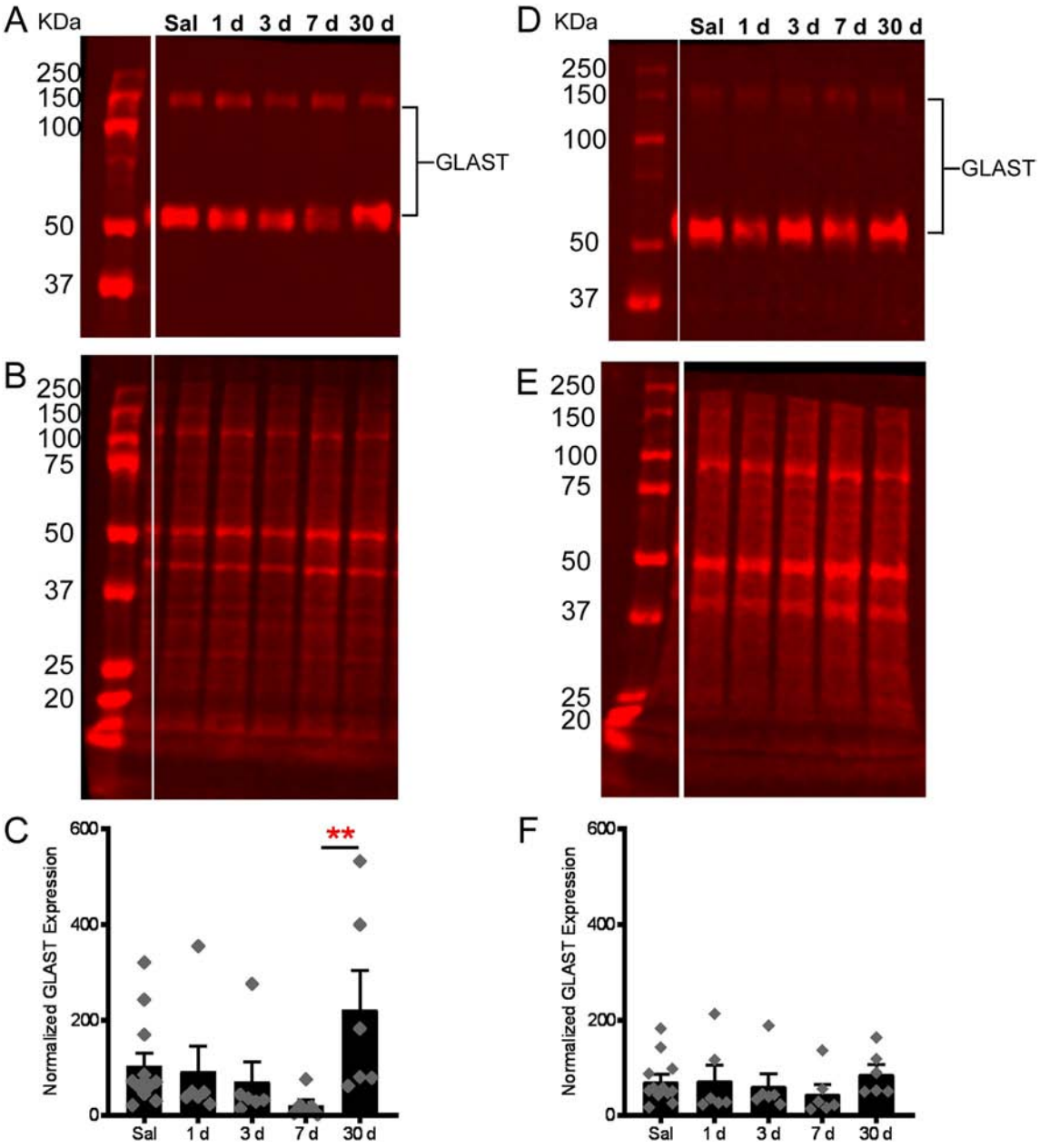

Fig. 11. Synaptosomal glutamate aspartate transporter (GLAST) expression in the IHKA model of epilepsy. A. Representative Western blot of GLAST in saline controls and 1, 3, 7 and 30 days post-SE in the ipsilateral dorsal hippocampus. B. Total protein stain indicating equivalent protein loading (5 μg) for ipsilateral dorsal hippocampus. C. Quantification of GLAST band intensities at each time point normalized to total protein stain in the ipsilateral dorsal hippocampus. D. Representative Western blot of GLAST in saline controls and 1, 3, 7, and 30 days post-SE in the contralateral dorsal hippocampus. E. Total protein stain indicating equivalent protein loading (5 μg) for contralateral dorsal hippocampus. F. Quantification of GLAST band intensities at each time point normalized to total protein stain in the contralateral dorsal hippocampus. For each time point post-IHKA, n = 6 animals were used. For saline-injected (control) n = 12 animals were used. ** indicates $P < .01$.

In summary, we demonstrate marked changes in astrocytic glutamate transporters, GLT-1 and GLAST, during epileptogenesis in the IHKA model of epilepsy. We showed that GLT-1 and GLAST immunoreactivity is increased in the hippocampus early after status epilepticus (1 and 3 days post-IHKA), but there is downregulation of synaptosomal GLT-1 protein in the early epileptogenic phase (7 days post-IHKA) corresponding to the onset of spontaneous seizures in this model. Future studies should examine the mechanisms responsible for GLT-1 downregulation and subcellular targeting, and the functional effects on glutamate uptake and excitability. Restoration of synaptic

Fig. 10. Quantification of glutamate aspartate transporter (GLAST) immunoreactivity in the contralateral dorsal hippocampus. Mean gray scale values shown at the indicated time points after kainic acid-induced status epilepticus. For each time point post-IHKA, n = 3 animals were used. For saline injections (controls), n = 5 animals were used.

glutamate homeostasis through modulation of astrocyte glutamate transport would be a novel therapeutic strategy for the treatment of epilepsy.

ACKNOWLEDGEMENTS

The authors would like to thank Dr. Meera Nair, Dr. Declan McCole and Dr. Djurdjica Coss (UCR) for the use of their Leica DM5500 fluorescence microscope, Dr. Jacqueline Hubbard for her synaptosomal fractionation protocol, Dr. Jonathan Lovelace for his assistance with statistical analysis, and Terese Garcia for her assistance with immunohistochemical quantification. This research did not receive any specific grant from funding agencies in the public, commercial, or not-for-profit sectors.

REFERENCES

Araque A, Parpura V, Sanzgiri RP, Haydon PG. (1999) Tripartite synapses: glia, the unacknowledged partner. Trends Neurosci 22:208-215.

Araque A, Carmignoto G, Haydon PG, Oliet SH, Robitaille R, Volterra A. (2014) Gliotransmitters travel in time and space. Neuron 81:728-739.

Barker-Haliski M, White HS. (2015) Glutamatergic mechanisms associated with seizures and epilepsy. Cold Spring Harb Perspect Med 5:a022863.

Bootsma HP, Ricker L, Hekster YA, Hulsman J, Lambrechts D, Majoie M, Schellekens A, de Krom M, Aldenkamp AP. (2009) The impact of side effects on long-term retention in three new antiepileptic drugs. Seizure 18:327-331.

Chen B, Choi H, Hirsch LJ, Katz A, Legge A, Buchsbaum R, Detyniecki K. (2017) Psychiatric and behavioral side effects of antiepileptic drugs in adults with epilepsy. Epilepsy Behav 76:24-31.

Danbolt NC. (2001) Glutamate uptake. Prog Neurobiol 65:1-105.

Danysz W, Parsons CG. (2012) Alzheimer's disease, beta-amyloid, glutamate, NMDA receptors and memantine – searching for the connections. Br J Pharmacol 167:324-352.

During MJ, Spencer DD. (1993) Extracellular hippocampal glutamate and spontaneous seizure in the conscious human brain. Lancet 341:1607-1610.

Evans GJ. (2015) Subcellular fractionation of the brain: preparation of synaptosomes and synaptic vesicles. Cold Spring Harb Protoc 2015:462-466.

Fisher RS, Acevedo C, Arzimanoglou A, Bogacz A, Cross JH, Elger CE, Engel J, Forsgren L, French JA, Glynn M, Hesdorffer DC, Lee BI, Mathern GW, Moshe SL, Perucca E, Scheffer IE, Tomson T, Watanabe M, Wiebe S. (2014) ILAE official report: a practical clinical definition of epilepsy. Epilepsia 55:475-482.

Foran E, Trotti D. (2009) Glutamate transporters and the excitotoxic path to motor neuron degeneration in amyotrophic lateral sclerosis. Antioxid Redox Signal 11:1587-1602.

Foran E, Rosenblum L, Bogush A, Pasinelli P, Trotti D. (2014) Sumoylation of the astroglial glutamate transporter EAAT2 governs its intracellular compartmentalization. Glia 62:1241-1253.

Huang K, Kang MH, Askew C, Kang R, Sanders SS, Wan J, Davis NG, Hayden MR. (2010) Palmitoylation and function of glial glutamate transporter-1 is reduced in the YAC128 mouse model of Huntington disease. Neurobiol Dis 40:207-215.

Hubbard JA, Hsu MS, Fiacco TA, Binder DK. (2013) Glial cell changes in epilepsy: overview of the clinical problem and therapeutic opportunities. Neurochem Int 63:638-651.

Hubbard JA, Szu JI, Yonan JM, Binder DK. (2016) Regulation of astrocyte glutamate transporter-1 (GLT1) and aquaporin-4 (AQP4) expression in a model of epilepsy. Exp Neurol 283:85-96.

Jacob CP, Koutsilieri E, Bartl J, Neuen-Jacob E, Arzberger T, Zander N, Ravid R, Roggendorf W, Riederer P, Grunblatt E. (2007) Alterations in expression of glutamatergic transporters and receptors in sporadic Alzheimer's disease. J Alzheimers Dis 11:97-116.

Jutila L, Immonen A, Mervaala E, Partanen J, Partanen K, Puranen M, Kalviainen R, Alafuzoff I, Hurskainen H, Vapalahti M, Ylinen A. (2002) Long term outcome of temporal lobe epilepsy surgery: analyses of 140 consecutive patients. J Neurol Neurosurg Psychiatry 73:486-494.

Kim K, Lee SG, Kegelman TP, Su ZZ, Das SK, Dash R, Dasgupta S, Barral PM, Hedvat M, Diaz P, Reed JC, Stebbins JL, Pellecchia M, Sarkar D, Fisher PB. (2011) Role of excitatory amino acid transporter-2 (EAAT2) and glutamate in neurodegeneration: opportunities for developing novel therapeutics. J Cell Physiol 226:2484-2493.

Kwan P, Brodie MJ. (2000) Early identification of refractory epilepsy. N Engl J Med 342:314-319.

Lee DJ, Hsu MS, Seldin MM, Arellano JL, Binder DK. (2012) Decreased expression of the glial water channel aquaporin-4 in the intrahippocampal kainic acid model of epileptogenesis. Exp Neurol 235:246-255.

Lepeta K, Lourenco MV, Schweitzer BC, Martino Adami PV, Banerjee P, Catuara-Solarz S, de La Fuente Revenga M, Guillem AM, Haidar M, Ijomone OM, Nadorp B, Qi L, Perera ND, Refsgaard LK, Reid KM, Sabbar M, Sahoo A, Schaefer N, Sheean RK, Suska A, Verma R, Vicidomini C, Wright D, Zhang XD, Seidenbecher C. (2016) Synaptopathies: synaptic dysfunction in neurological disorders - a review from students to students. J Neurochem 138:785-805.

Levesque M, Avoli M. (2013) The kainic acid model of temporal lobe epilepsy. Neurosci Biobehav Rev 37:2887-2899.

Lin CL, Bristol LA, Jin L, Dykes-Hoberg M, Crawford T, Clawson L, Rothstein JD. (1998) Aberrant RNA processing in a neurodegenerative disease: the cause for absent EAAT2, a glutamate transporter, in amyotrophic lateral sclerosis. Neuron 20:589-602.

Medina-Ceja L, Pardo-Pena K, Morales-Villagran A, Ortega-Ibarra J, Lopez-Perez S. (2015) Increase in the extracellular glutamate level during seizures and electrical stimulation determined using a high temporal resolution technique. BMC Neurosci 16:11.

Munoz-Ballester C, Berthier A, Viana R, Sanz P. (2016) Homeostasis of the astrocytic glutamate transporter GLT-1 is altered in mouse models of Lafora disease. Biochim Biophys Acta 1862:1074-1083.

Ngugi AK, Bottomley C, Kleinschmidt I, Sander JW, Newton CR. (2010) Estimation of the burden of active and life-time epilepsy: a meta-analytic approach. Epilepsia 51:883-890.

Postupna NO, Keene CD, Latimer C, Sherfield EE, Van Gelder RD, Ojemann JG, Montine TJ, Darvas M. (2014) Flow cytometry analysis of synaptosomes from post-mortem human brain reveals changes specific to Lewy body and Alzheimer's disease. Lab Invest 94:1161-1172.

Proper EA, Hoogland G, Kappen SM, Jansen GH, Rensen MG, Schrama LH, van Veelen CW, van Rijen PC, van Nieuwenhuizen O, Gispen WH, de Graan PN. (2002) Distribution of glutamate transporters in the hippocampus of patients with pharmaco-resistant temporal lobe epilepsy. Brain 125:32-43.

Racine RJ. (1972) Modification of seizure activity by electrical stimulation. II. Motor seizure. Electroencephalogr Clin Neurophysiol 32:281-294.

Raedt R, Van Dycke A, Van Melkebeke D, De Smedt T, Claeys P, Wyckhuys T, Vonck K, Wadman W, Boon P. (2009) Seizures in the intrahippocampal kainic acid epilepsy model: characterization using long-term video-EEG monitoring in the rat. Acta Neurol Scand 119:293-303.

Rizo J, Sudhof TC. (2002) Snares and Munc18 in synaptic vesicle fusion. Nat Rev Neurosci 3:641-653.

Sankaraneni R, Lachhwani D. (2015) Antiepileptic drugs–a review. Pediatr Ann 44:e36-e42.

Schreiner AE, Durry S, Aida T, Stock MC, Ruther U, Tanaka K, Rose CR, Kafitz KW. (2014) Laminar and subcellular heterogeneity of GLAST and GLT-1 immunoreactivity in the developing postnatal mouse hippocampus. J Comp Neurol 522:204-224.

Sheng M, Sala C. (2001) PDZ domains and the organization of supramolecular complexes. Annu Rev Neurosci 24:1-29.

Singh A, Trevick S. (2016) The epidemiology of global epilepsy. Neurol Clin 34:837-847.

Soukupova M, Binaschi A, Falcicchia C, Palma E, Roncon P, Zucchini S, Simonato M. (2015) Increased extracellular levels of glutamate in the hippocampus of chronically epileptic rats. Neuroscience 301:246-253.

Sugimoto J, Tanaka M, Sugiyama K, Ito Y, Aizawa H, Soma M, Shimizu T, Mitani A, Tanaka K. (2018) Region-specific deletions of the glutamate transporter GLT1 differentially affect seizure activity and neurodegeneration in mice. Glia 66:777-788.

Tanaka K, Watase K, Manabe T, Yamada K, Watanabe M, Takahashi K, Iwama H, Nishikawa T, Ichihara N, Kikuchi T, Okuyama S, Kawashima N, Hori S, Takimoto M, Wada K. (1997) Epilepsy and exacerbation of brain. Injury in Mice Lacking the Glutamate Transporter GLT-1. 276. , 19971699-1702.

Tessler S, Danbolt NC, Faull RL, Storm-Mathisen J, Emson PC. (1999) Expression of the glutamate transporters in human temporal lobe epilepsy. Neuroscience 88:1083-1091.

Thom M. (2014) Review: hippocampal sclerosis in epilepsy: a neuropathology review. Neuropathol Appl Neurobiol 40:520-543.

Valencia A, Sapp E, Kimm JS, McClory H, Ansong KA, Yohrling G, Kwak S, Kegel KB, Green KM, Shaffer SA, Aronin N, DiFiglia M. (2013) Striatal synaptosomes from Hdh140Q/140Q knock-in mice have altered protein levels, novel sites of methionine oxidation, and excess glutamate release after stimulation. J Huntingtons Dis 2:459-475.

Zhang Y, He X, Meng X, Wu X, Tong H, Zhang X, Qu S. (2017) Regulation of glutamate transporter trafficking by Nedd4-2 in a Parkinson's disease model. Cell Death Dis 8:e2574.

(Received 23 March 2019)
(Available online 31 May 2019)